Synthesis and characterization of molecularly imprinted silica for efficient adsorption of melamine

Ferdaous Arfaoui[a,b], Najeh Jaoued-Grayaa[a], Akila Riani Khlifi[c] and Rafik Kalfat[a] *

[a)] *Laboratoire Matériaux, Traitement et Analyse, Institut National de Recherche et d'Analyse Physico-chimique, BiotechPole Sidi-Thabet, 2032 Ariana, Tunisie.*
[b)] *Université Tunis El Manar, Faculté des Sciences de Tunis, Campus Universitaire Farhat Hached, 1068-Tunis, Tunisie.*
[c)] *Research center in microelectronics and nanotechnology, Techpole of Sousse, Sahloul (BP 334 Sahloul, Sousse)*

(Received: 23 September 2016, accepted: 20 June 2017)

Abstract: We report on the elaboration of a new melamine molecularly imprinted silica (MIP). It was synthesized by surface molecular imprinting technique using silica gel as rigid support. Melamine was used as template molecule, 3-mercaptopropyl trimethoxysilane immobilized onto the silica gel surface was used as a functional monomer and tetraethoxysilane (TEOS) as crosslinker. A non imprinted polymer was used (NIP) for comparison. The prepared materials were characterized by FT-IR, ATG and BET. The batch binding tests were carried out to evaluate the adsorption kinetics and adsorption isotherms either for MIP and NIP. Results show that the imprinted sorbent exhibits higher binding capacity toward Melamine (Q_{max} = 912 µg.g^{-1}) compared to the non-imprinted one (Q_{max} = 338 µg.g^{-1}). Two binding isotherm models (Langmuir and Freundlich) were used to check the adsorption mode. The Freundlich model appears as the most suitable model for both imprinted and non-imprinted materials.The adsorption kinetic data were modeled using the pseudo-first and pseudo-second order equations. The results indicated that the adsorption of MEL on MIP follows a pseudo-second-order kinetic. Differentiation between adsorption phenomena onto each of the two substrates has been proposed and compared to the theoretical classification of adsorption isotherms. The application of intraparticle diffusion kinetics model has indicated that intraparticle diffusion was not the only rate limiting mechanism in the adsorption process.

Keywords: Melamine, Molecularly Imprinted Polymer, silica gel.

INTRODUCTION

The molecularly imprinted polymers (MIPs) have already proved their effectiveness to act as biomimetic receptors. These materials present high affinity and selectivity for the separation of different molecules owing to their recognition properties [1]. The majority of the produced MIPs are based on acrylic polymers and were investigated in analysis of specific molecules contained in real matrix [2,3]. Such materials were used in different applications including electrochemical sensor [4-6], SPE [7-9] and SPME [10,11]. A part from their demonstrated selectivity, acrylic MIPs preparation requires grinding and sieving steps to obtain homogenous particles which can damage the recognition cavities. In addition, this kind of polymers requires complex conditions: inert atmospheric conditions and incorporating non-polar solvents acting as porogen [12]. This further excludes the use of template molecules that are only soluble in polar solvents [13]. So, sol-gel imprinting route represents a good alternative that meets the requirements for the formation homogenous particles and the recognition of hydrophilic target molecules. Sol-gel process has been one of the emerging technologies in the synthesis of inorganic polymers and organic-inorganic hybrid materials [14]. Some research teams have prepared hybrid imprinted sorbents, to separate different target molecules, by sol-gel process involving silane based monomers [15,16]. The preparation of the hole inorganic or organic-inorganic adsorbing material, starting from pure metallic alkoxydes is quite expensive owing

* Corresponding author, e-mail address : rafik.kalfat@gmail.com, Tel: +216 71 537 666, Fax: +216 71 537 688

to the fact that only a thin external layer of the produced particles is really implicated in the separation phenomenon, the core of the adsorbent particle remains inaccessible by the analyte species.

The grafting of molecular imprinting polymer onto the surface of solid particles presents an interesting alternative coming back to origin of imprinting process. In fact, the first "molecular imprinting" was observed in 1931 by Polvakov [17]. Then, Pauling applied this theory to investigate the adsorption characteristics of alkyl orange dyes-imprinted silica and the results were reported by his student Dickey [18]. In their study, the imprinting effect onto silica was demonstrated clearly. Owing to its definite advantages, such as deforming resistance and good mechanical rigidity and heat-stability, silica gel could be adopted in imprinting media as a solid support [19]. In the present work, sorbent materials were prepared by surface polymerization using the sol-gel route. The use of organofunctional silanes as precursors in a sol-gel process results in the formation of an organically modified hybrid material with highly cross-linked structure, stifness and flexibility of the MIP and readly acheives useful surface functions for the establishment of interactions with the molecule model [20]. Furthermore, the distance between the crosslinks in the silica is much lower than in organic polymers, which exhibits a minimal swelling in the presence of solvents and shows excellent thermal stability. Melamine, the target molecule used in this study, is soluble only in polar solvents [21-23]. Hence, the prepared MIP for the recognition of melamine was achieved in polar solvent allowing a good dissolution of total amount of melamine introduced in the course of synthesis.

The mercaptopropyl-triethoxysilane (MPTMS) presents a terminal thiol group (electron acceptor) favoring the establishment of hydrogen bonding interaction with amine groups (electron donors) of melamnine leading to the formation of a pre-polymerization complex. Some studies have demonstrated that there exists a hydrogen bonding interaction between alkyl thiol and amine and that this interaction is strong enough to be considered in a polar solvent [24-26].

The MPTMS was grafted onto silica surface and used as functional monomer and the tetraethoxysilane was used as the crosslinker. The adsorption model of melamine onto the imprinted and the non-imprinted materials were assessed by adsorption isotherms. Adsorption kinetic parameters were established through kinetic measurements.

EXPERIMENTAL

1 Chemicals

Silica gel (70-230 mesh) was used as support for the preparation of surface imprinted silica. Melamine was purchased from Aldrich, 3-(mercaptopropyl)-trimethoxysilane (MPTMS) was obtained from Sigma-Aldrich (Steinheim, Germany), methanol and acetic acid (HAc) from CARLO ERBA and toluene from LOBA Chemie. Silica gel and tetraethoxisilane (TEOS) were purchased from Fluka Analytical.

2. Instrumentation

The FT-Raman spectrum was recorded using Jobin-Yvon spectrometer (T64000 model) equipped with an Ar + lazer (λ_{ex} = 488 nm) and a CCD detector in a back-scattering geometry.

Thermal analysis of samples was performed using a thermogravimetric analyser (TG model, TA instruments SETERAM. SETSYS 1750).

Elemental analyses of C, H and N was carried out with a Perkin Elmer CHN-2400 instrumentation and S analysis with a Sulfur Analyzer EMIA.

Brunauer-Emmert-Teller (BET) and Barrett-Joyner -Halenda (BJH) measurements was assessed through N_2 adsorption at 77 K using an automatic physisorption analyser TRISTAR 3000.

The adsorption tests were performed using High Performance Liquid Chromatography (HPLC) technique using Agilent-HPLC equipment, equipped with a DAD UV/vis Detector (set at 208 nm). The chromatographic separation was carried out with a Asahipak NH_2P-50 4E column (250 × 4.6 mm, 5 µm) using acetonitrile-water (75: 25, v/v) as mobile phase. The column was maintained at room temperature with a flow rate of 0.3 mL.min^{-1}.

3. Synthesis of Imprinted MEL sorbent:

The synthesis of molecularly imprinted sol-gel is carried out in two separate steps by sol-gel process (Fig.1).

The silica gel (15 g) was slurried in anhydrous toluene (80 mL) then heated at reflux for 3 h using a Dean–Stark trap in order to remove the water adsorbed on the surface. After cooling down to room temperature, the 3-MPTMS (7.4 g) was added and the suspension was heated up to 110°C

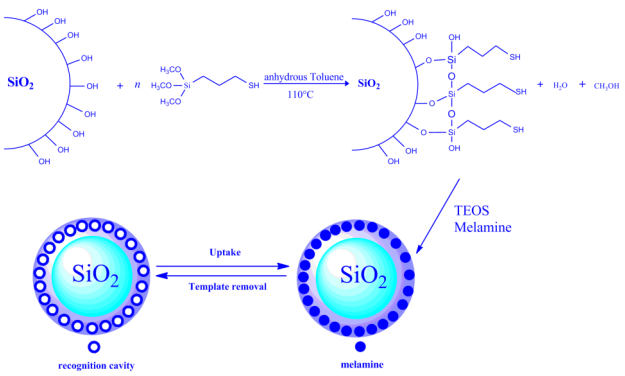

Fig.1: Schematic MIP@SiO2 synthesis

under nitrogen for 72 h. The resulted functionalized silica was filtered, washed with toluene and methanol and dried overnight under vaccum at 60°C. An amount of 730 mg of functionalized silica was dispersed with 30 mg of MEL in 50 mL of methanol and the mixture was stirred for 12 hours. Then 446 mg (0,23 mmol) of TEOS was added and the mixture was heated to 40°C for 24 h. The ratio template/functional monomer/cross linker was chosen as (1/6/10). The obtained material was filtered, washed three times with methanol and dried in oven at 60°C for 12 h. MEL was removed by soxhlet extraction apparatus with a mixture of methanol and acetic acid (1/9) (V/V) for 48 h, then the powder was washed with acetone and dried at 80°C for 24 h.

A non-imprinted sol-gel (NIP@SiO_2) was prepared under identical conditions in the absence of the template.

4. Adsorption experiments studies

The adsorption isotherms of MEL by MIP and NIP were performed to determine the adsorption capacities of the adsorbents. In static adsorption tests, 2 mL of MEL standard solutions (1ppm-20ppm) was added to 10 mg of adsorbent (MIP@SiO_2 or NIP@SiO_2) placed in 5 mL vials. The mixture was shaken for 1h at 25°C then the solution was centrifuged at 3000 rpm for 15 min and the supernatant of each solution was collected. Then the free concentrations of MEL were determined with HPLC. Meanwhile, the dynamic binding test was carried out in a similar way except that the initial concentration was constant (10 mg.L^{-1}) and the measurements were taken at different time range (5 min, 10 min, 15 min, 20 min, 25 min, 30 min, 45 min, 60 min and 120 min).

The adsorption amount of both imprinted and non-imprinted silica (Q) was calculated according to the following equation (Eq(1)) [7].

$$Q = \frac{(co-cf)\,v}{m} \qquad \textbf{Eq (1)}$$

Where Q (mg.g^{-1}) is the amount of total adsorption of MEL, C_0 (mg.L^{-1}) and C_f (mg.L^{-1}) are the initial and final concentration of MEL in solution, respectively, V (L) is the total volume of the solution and m (mg) is the weight of sorbent.

The adsorption isotherms were described by the Langmuir equation (Eq. (2)) and the Freundlich equation [27] (Eq. (3))

$$1/Q_e = 1/Q_m + 1/(Q_m K_L C_e) \qquad \textbf{Eq (2)}$$

$$\log Qe = \log K_F + 1/n \,.\, \log Ce \qquad \textbf{Eq (3)}$$

where Ce (mol.L^{-1}) and Q_e are the equilibrium concentration of MEL and the amount of MEL adsorbed per gram of sorbent (mol.g^{-1}) at equilibrum, respectively. Q_m (mg.g^{-1}) is the theoretically saturatedadsorption capacity of MEL and K_L (L.g^{-1}) is the Langmuir adsorption equilibrium constant. K_F and n are the Freundlich constants, which are indicators of adsorption capacity and the implicated adsorption phenomenon respectively.

RESULTS AND DISCUSSION

1. Chemical and structural characterization of MIP@SiO_2

1.1. Infrared and Raman spectroscopy

FTIR spectra of MPTMS@SiO_2 (Fig.2.a) and MIP@SiO_2 before (Fig.2.b) and after (Fig.2.c) melamine removal show characteristic peaks.

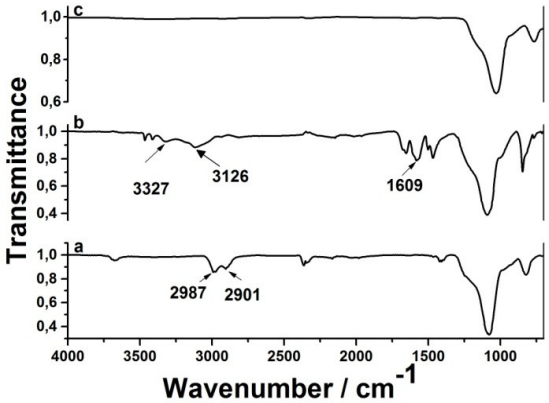

Fig.2: IR spectra of MPTMS-SiO_2 (a), MIP@SiO_2 before (b) and after (c) melamine removal

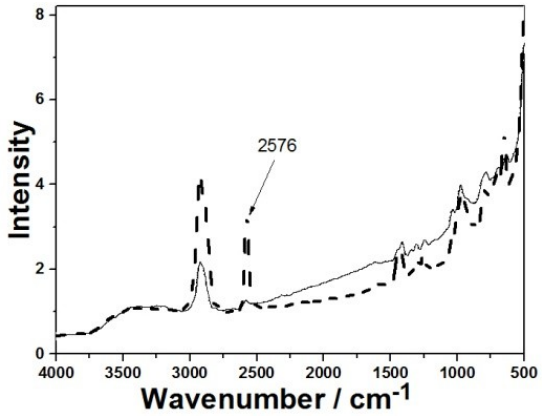

Fig.3: Raman spectrum of MPTMS@SiO_2 (Dash line) and MIP@SiO_2 after template removal (straight line)

The strong absorption band at 1192 cm^{-1} and 1050 cm^{-1} are assigned to the asymmetric stretching vibrationof Si-O-Si. These bands are characteristic of silica network, they arise from siloxane bonds and are common for the three materials. The MPTMS@SiO_2 IR spectrum shows stretching vibration bands (ν_{sym} 2901 cm^{-1} and ν_{asym} 2987 cm^{-1}) relative to CH_2 groups of MPTMS grafted onto silica surface. S-H stretching vibration of MPTMS is more intense in Raman spectrum [28] and appears at 2576 cm^{-1} in Fig.3. The spectrum of MIP@SiO_2 before melamine removal (Fig.2.b) displayed characteristic peaks of melamine. The peaks observed at 3327 cm^{-1}, 3126 cm^{-1} and 1609 cm^{-1} are attributed to the stretching vibration of NH_2, N-H, and C=N of melamine [29] respectively. These peaks disappear in the spectrum of MIP@SiO_2 after template removal, suggesting that the melamine was successfully removed from MIP which was further proved by Raman spectrum that shows only the S-H stretching vibration at 2576 cm^{-1} and stretching vibration bands relative to CH_2 groups.

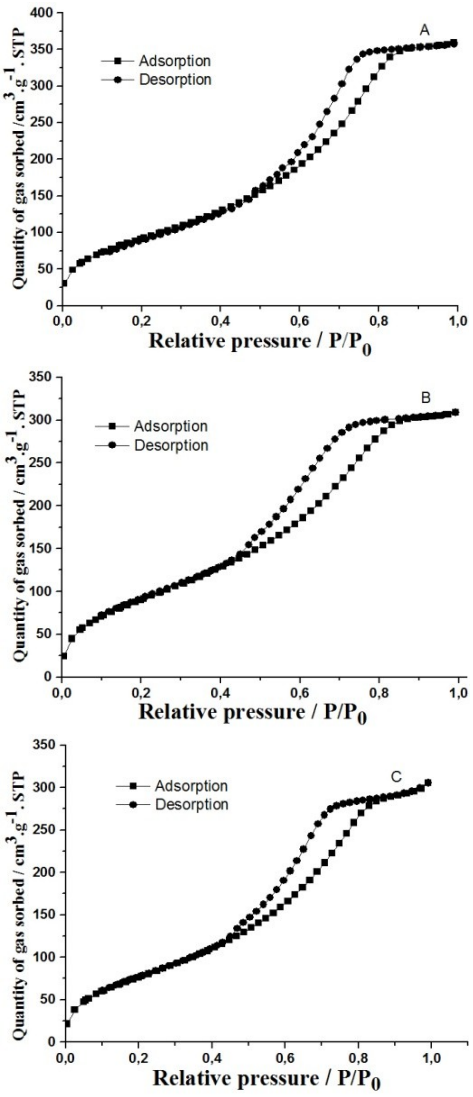

Fig.5: Nitrogen adsorption-desorption isotherms MPTMS@SiO_2 (A), NIP@SiO_2 (B) and MIP@SiO_2 (C)

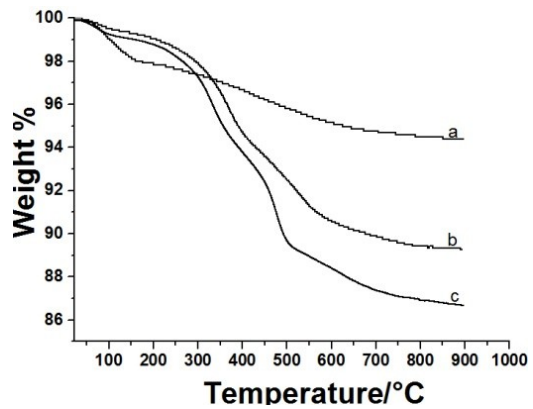

Fig.4: TGA curves of silica gel (a), MPTMS-SiO_2 (b) and MIP@SiO_2 before melamine removal (c)

1.2 Thermogravimetric analysis

TGA curves of bare silica, MPTMS-SiO_2 and MIP@SiO_2 before template removal are shown in Fig.4.

The TGA curve of bare silica gel shows a net weight loss between 25°C and 100°C corresponding to the release of physically adsorbed water onto silica surface.

The TGA curve of functionalized silica (Fig.4.b) exhibited a slight decrease between 25°C and 150°C,

attributed to the removal of both residual adsorbed water and ethanol resulting from MPTMS alcoxysilane condensation. The weight losses between 270°C and 800°C, correspond to the degradation of organic moieties coming from MPTMS grafted onto silica surface. The coverage ratio of MPTMS grafted onto silica surface, estimated from the recorded weight losses, was 1.17 mmol.g^{-1}. The grafting degree, calculated from elemental analysis using Eq(4), gives a value of the same magnitude 1.8 mmol.g^{-1}. The TGA curve of MIP@SiO_2 (Fig.4.c) presents the same shape than that of MPTMS@SiO_2, but the two second weigtht losses in the range 350°C-800°C (9%) are higher than that of MPTMS-SiO_2 (6%). This difference in weight loss (Δw =3%) corresponds to the template mass ratio present in the MIP@SiO_2 matrix which is close to the theoretical data (3.66 %), representing the template weight percentage used for the preparation of MIP@SiO_2.

$$\frac{1000 \times \%S}{3200 - \%S \times MWgc} \qquad \textbf{Eq (4)}$$

1.3. BET measurements

The nitrogen adsorption-desorption analysis of MPTMS@SiO_2, MIP@SiO_2 and NIP@SiO_2 were done to investigate the changes of pore structure. Figure 5 shows that the three materials exhibited typical "type IV" isotherms (with the presence of hysteresis) according to the IUPAC classification, indicative of a mesoporous material.

The MIP@SiO_2 exhibited larger pore diameters (5.132 nm) than NIP@SiO_2 (4.702 nm). Similar results were reported by Kulsing et al [30] who suggested that the formation of larger pore structure in the imprinted silica could arise from the removal of the template.

Table I: The total pore volume and pore diameters of MIP@SiO_2 and NIP@SiO_2

Sample	V_a(cm^3.g^{-1})	dp(nm)
MIP@SiO_2	0.43	5.1
MPTMS@SiO_2	0.51	5.1
NIP@SiO_2	0.41	4.7

Large porosity distribution is observed in functionalized silica (Fig.6). A net bimodal distribution of pore size appears in the polymer coated silica either for MIP@SiO_2 or NIP@SiO_2. Figure 6 shows the presence of small size pores with narrow diameter distribution centred at 3 nm also with a larger size pores with a wider size distribution for MIP@SiO_2.

Parameters of pore structure of the materials are given in Table I. The MIP@SiO_2 shows the same pore diameter than the functionalized MTPMS@SiO_2 but with a smaller pore volume suggesting the presence of superficial shallow pores.

2. Adsorption characteristic of MIP@SiO_2 and NIP@SiO_2

2.1. Kinetic studies

The kinetic adsorption test of MIP@SiO_2 and NIP@SiO_2 was investigated in different time intervals (5 min-120 min). The adsorption kinetic curves of MIP@$SiO_2$and NIP@SiO_2 are shown in Fig.7. The amount of melamine adsorbed by both materials increased with time. At the beginning of

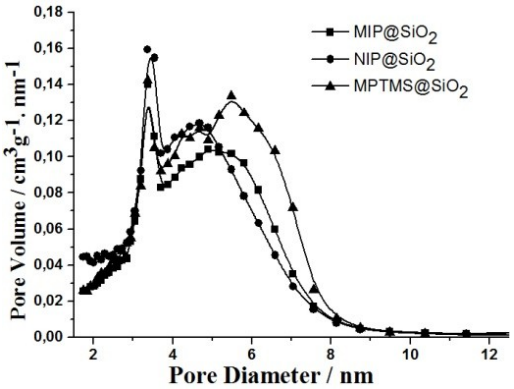

Fig.6: Pore size distribution of MPTMS@SiO_2, NIP@SiO_2 and MIP@SiO_2

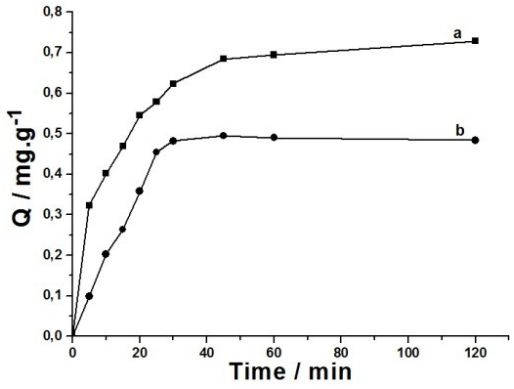

Fig.7: Dynamic adsorption curves of MIP@SiO_2 (a) and NIP@SiO_2 (b)

Table II: Pseudo-first-order and pseudo-second-order adsorption kinetic constants

Experimental	Pseudo-first-order model			Pseudo-second-order model		
$q_{e\ (exp)}$ [mg.g^{-1}]	$q_{e\ cal}$ [mg.g^{-1}]	k_1 [min^{-1}]	R^2	$q_{e\ cal}$ [mg.g^{-1}]	k_2 [g.mg^{-1}.min^{-1}]	R^2
0.730	1.520	0.371	0.948	0.860	0.098	0.990

adsorption process, MIP shows a faster solute adsorption aptitude than NIP. Both materials reached a steady state within 60 min. Therefore, the adsorption time was set at 60 min for the subsequent static adsorption tests.

The rate constant of adsorption is calculated from the pseudo-first-order equation given by Langergren and Svenska [31] as equation 5 (Eq(5)):

$$\text{Ln}\ (q_e - q_t) = \text{Ln}\ q_e - k_1\, t \qquad \textbf{Eq (5)}$$

where q_e and q_t are the amounts of MEL adsorbed (mg.g^{-1}) at equilibrium and at time t (min), respectively, and k_1 (min^{-1}) is the rate constant of adsorption. The linear plot *Ln* $(q_e - q_t)$ against *t*, has allowed to extract the values of k_1 and q_e. The value of calculated q_e for MIP did not agree with the corresponding experimental value (Table II), suggesting that the pseudo-first-order kinetic model is not applicable for the imprinted material. Based on these results, the adsorption kinetics were further analyzed by the pseudo-second-order equation [31-33] (Eq (6))

$$t/q_t = 1/(k_2 q_e^2) + (1/q_e)\, t \qquad \textbf{Eq (6)}$$

where k_2 (g.min^{-1}.mg^{-1}) is the rate constant of second-order adsorption. It was found that the regression coefficient of the linear plot t/q_t against t for MIP (Table II) was high and the calculated q_e is closer to the corresponding experimental value, thus suggested that the pseudo-second-order model is more suitable to describe the adsorption process of MEL onto MIP.

As the above two kinetic models are not able to clarify the diffusion mechanism, thus intraparticle diffusion kinetic model based on the Weber-Moris equation (Eq (7)) was used to investigate the mechanism of adsorption [31, 32].

$$q_t = k_{di}\, t^{1/2} + C_i \qquad \textbf{Eq (7)}$$

where k_{di} is the rate parameter during stage i (mg.g^{-1}.min$^{1/2}$) obtained from the slope of straight line of q_t against $t^{1/2}$ (Fig.8). C_i is the intercept during stage i. It informs us about the thickness of the boundary layer particularly. The plot q_t against $t^{1/2}$ shows three linear portions, implying that three different adsorption steps take place.

The lines of second and third steps did not pass through the origin. This deviation from origin might be due to the difference in the mass transfer rate in the initial and final stages of adsorption. It shows that intraparticle diffusion was not the only rate limiting [33] mechanism in the adsorption process. Three sequential steps can be proposed. The first step is related to the film diffusion phenomenon, where absorbate molecules go across the external surface of MIP@SiO_2. The second step is related to an intraparticle diffusion phenomenon, where adsorbate molecules penetrate deeply into the core of the material. This stage represents a rate-limiting step of the whole phenomenon. The third step corresponds to the final steady state where the MEL molecules finally attain the proper site of adsorption. Table III shows the intraparticle diffusion rate parameters of the adsorption of MEL on MIP.

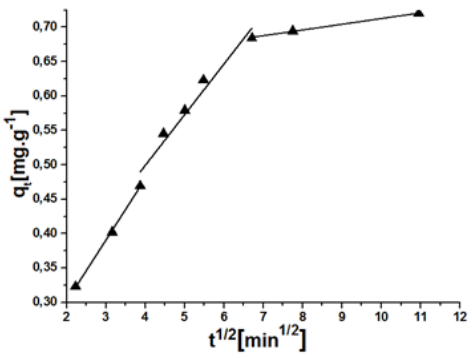

Fig.8: Intraparticle diffusion kinetics for adsorption of MEL onto MIP@SiO_2

Table III: Intraparticle diffusion constants and correlation coefficients for adsorption of MEL onto MIP@SiO_2

Intraparticle diffusion model*								
k_{d1}	k_{d2}	k_{d3}	C_1	C_2	C_3	$(R_1)^2$	$(R_2)^2$	$(R_3)^2$
0.089	0.073	0.008	0.122	0.204	0.62	0.999	0.980	0.999

*k_d in $mg.g^{-1}min^{1/2}$

2.2. Static binding test

Adsorption isotherm was studied to estimate the adsorption capacity of MEL on the MIP@SiO_2 and NIP@SiO_2. The adsorption capacity of MEL by MIP@SiO_2 and NIP@SiO_2 are represented in Fig.9. The adsorption capacity significantly increases at the beginning, with the increase of melamine concentration, when the Mel-imprinted MIPs shows much higher adsorption ability than the NIP for all concentration ranges. The maximum adsorption capacity of MIP@SiO_2 and NIP@SiO_2 were 912 $\mu g.g^{-1}$, and 338 $\mu g.g^{-1}$ respectively which are higher compared to the maximum capacity of 250 $\mu g.g^{-1}$, reached with melamine-MIP based on purely organic polymers made from bulk polymerization method using methacrylic acid (MAA) and ethylene glycol dimethacrylate (EGDMA) [8]. Adsorption isotherm of MEL in water with MIP and NIP give an S-type and C-type curve, respectively, according to Giles classification [34]. The S-schape of adsorption isotherm observed with MIP substrate is indicative of the formation of strong and cooperative adsorption. The presence of two plateaus in the isotherm curve (Fig.9.a) suggests the presence of two kinds of adsorption sites: unspecific and specific pores. After normal adsorption on the former is complete, the solute begins to penetrate into the specific pores.

The NIP subtrate gives a C-shape isotherm indicating that this material presents a relatively low accessible internal adsorption areas comparing with the external area. The ratio of maximum adsorption capacity of MIP@SiO_2 and NIP@SiO_2 allowed the calculation of the imprinting factor using equation 8 (Eq(8)) [35, 36].

$$\alpha = Q_{m(MIP)} / Q_{m(NIP)} \qquad \textbf{Eq (8)}$$

The calculated imprinting factor value was 2.69. This difference between adsorption ability of two sorbents suggests the presence of specific cavities in the MIP. The affinity of NIP against the template is related to the unspecific sites.

The adsorption isotherm data were fitted with Langmuir and Freundlich models, Fig.10 and Fig.11, respectively to estimate the binding properties of imprinted and non-imprinted adsorbents.

The plot 1/Qe versus 1/Ce was used to check for the Langmuir isotherm model. The linear regression equation for MIP@SiO_2 was

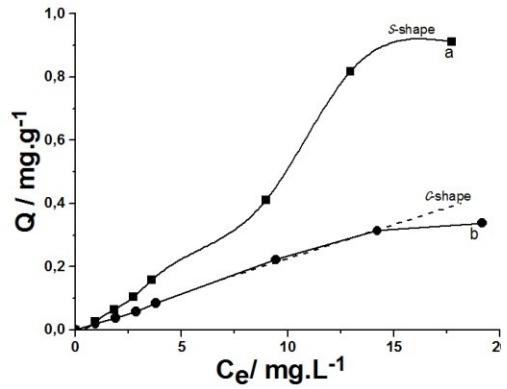

Fig 9: Static adsorption curve of MIP@SiO_2 (a) and NIP@SiO_2 (b)

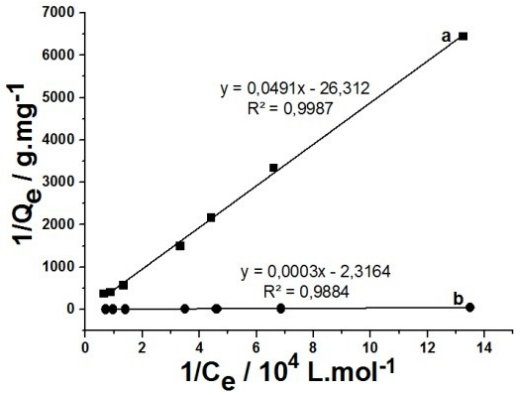

Fig.10: Langmuir isotherm of NIP@SiO_2 (a) and MIP@SiO_2 (b)

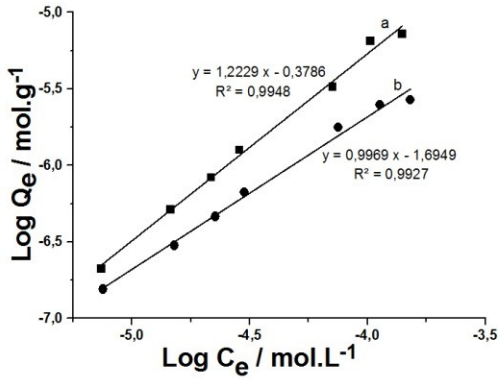

Fig.11: Freundlich isotherm of MIP@SiO_2 (a) and NIP@SiO_2 (b)

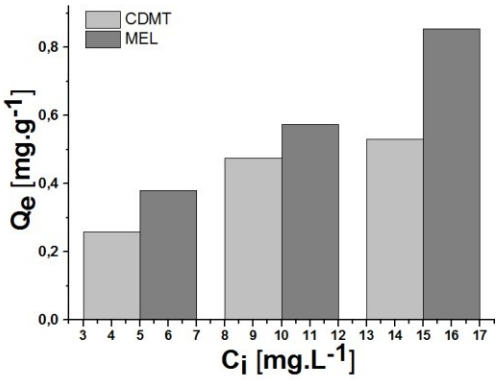

Fig.13: Adsorption capacities of MIP@SiO_2MA for MEL or CDMT

$y = 3.10^{-4} x - 2.316$ ($R^2 = 0.9884$). The plot log Qe versus log Ce was used to check for the Freundlich adsorption model. The linear regression equation obtained for MIP@SiO_2 was as $y = 1.2229 x - 0.378$ ($R^2 = 0.9948$), indicating that the Freundlich isotherm model was more suitable for the fitting of experimental data indicating that the adsorption, in this case, was accomplished within a multilayer arrangement. The estimated value of 1/n in Freundlich equation (Eq(3)) is above one (1/n = 1.22), suggesting the establishment of a cooperative adsorption phenomenon [25]. K_F value which represents an approximate indicator of adsorption capacity, was 0.418 $mol.g^{-1}$ corresponding to $2.51.10^{20}$ $molecule.mg^{-1}$.

For NIP@SiO_2, the linear regression equations of Langmuir and Freundlich isotherms (Fig.10.b and Fig.11.b) were described as $y = 0.0491 x - 26.312$ ($R^2 = 0.9987$) and that $y = 0.9969 x - 1.695$ ($R^2 = 0.9927$), respectively, indicating that the Freundlich isotherm model was more convenient for the experimental data suggesting that the adsorption of MEL with NIP@SiO_2 was accomplished by formation of multilayer. The value of 1/n is bellow one (1/n = 0.9969) which indicates normal adsorption phenomenon. The weak value of K_F (0.02 $mol.g^{-1}$) shows the reduced adsorption capacity of NIP compared to that of MIP.

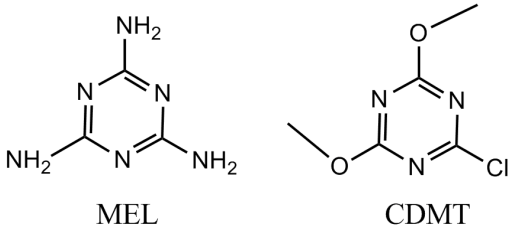

MEL CDMT

Fig.12: Chemical structure of MEL and CDMT

2.3. Selectivity test

In order to demonstrate the selective character of the MIP@SiO_2 towards melamine (MEL), we used the 2-chloro-4,6-dimethoxy-1,3,5-triazine (CDMT) as interfering, whose structures are represented in fig.12. Respectively, 10 µl of solution containing a certain concentration (5ppm, 10 ppm and 15 ppm) of MEL and CDMT were added to MIP@SiO_2. After stirring the supernatant was analysed by UV spectrometer. Fig. 13 shows that the adsorption capacity of MEL is 0,38-0,85 $mg.g^{-1}$, while the adsorption capacity of CDMT is only 0,25-0,53 $mg.g^{-1}$, the above results clearly revealed that MIP@SiO_2 possessed high recognition selectivity and binding affinity against MEL.

CONCLUSION

In this work, a simple molecular imprinting procedure was developed for the preparation of melamine imprinted silica gel sorbent. Sol-gel process was used owing to its simplicity and to the low-cost silica gel that was selected as a rigid matrix for the surface coating of MIP or NIP. The static adsorption tests have shown the higher adsorption capacity of imprinted silica against melamine. The Freundlich model was more adapted than Langmuir for fitting experimental adsorption data. The kinetic adsorption process was more described by the pseudo-second-order equation and intraparticle diffusion model.

Acknowledgement: The research in our laboratory has been enriched by past and present collaborators and members, especially: M. Y. Chevalier is gratefully acknowledged for his guidance and support. The Director of LAGEP laboratory in Claude Bernard Lyon1 University, is also acknowledged for experimental facilities during the traineeship of Miss F. Arfaoui.

REFERENCES

[1] G. Vasapollo, R. Del Sole, L. Mergola, MR. Lazzoi, A. Scardino, S. Scorrano, G.Mele. **2011,** *Int J Mol Sci*. Molecularly Imprinted Polymers: Present and Future Prospective. **12:** 5908‑5945.

[2] R.G. Da Costa Silva, F. Augusto. **2006**, *J. Chromatogr. A.* Sol-gel molecular imprinted ormosil for solid‑phase extraction of methylxanthines. **1114:** 216-223.

[3] G. Cirillo, M. Curcio, O.I. Parisi, F. Puoci, F. Iemma, U.G. Spizzirri, D. Restuccia, N. Picci. **2011**, *Food Chem*. Molecularly imprinted polymers for the selective extraction of glycyrrhizic acid from liquorice roots. **125:** 1058‑1063.

[4] Y. Mao, Y. Bao, S. Gana, F. Li, L. Niu. **2011**, *Biosens Bioelectron*. Electrochemical sensor for dopamine based on a novel graphene-molecular imprinted polymers composite recognition element. **28:** 291-297.

[5] D. Lakshmi, A. Bossi, M.J. Whitcombe, I. Chianella, S. A. Fowler, S. Subrahmanyam, E.V. Pilestska, S.A. Piletsky. **2009**, *Anal Chem.* Elechtrochemical sensor for catechol and dopamine based on a molecularly imprinted catalytic polymer-conducting polymer hybrid recognition element. **81:** 3576‑3584.

[6] A. Khlifi, S.Gam-. Derouich, M. Jouini, R. Kalfat, M.M. Chehimi. **2013**, Food Control. Melamine-imprinted polymer grafts through surface photopolymerization initiated by aryl layers from diazonium salts. **31:** 279-386.

[7] J. Liu, H. Song, J. Liu, Y. Liu, L. Li, H. Tang, Y. Li. **2015**, *Talanta.* Preparation of molecularly imprinted polymer with double templates for rapid simultaneous determination of melamine and dicyandiamide in dairy. **134:** 761-767.

[8] H-H. Yang, W.H. Zhou, X.C. Guo, F.R. Chen, H.Q. Zhao, L.M. Lin, X.R. Wang. **2009**, *Talanta.* Molecularly imprinted polymer as SPE sorbent for selective extraction of melamine in dairy products. **80:** 821-825.

[9] M. Li, L. Zhang, Z. Meng, Z. Wang, H. Wu. **2010**, *J Chromatogr B.* Molecularly-imprinted microspheres for selective extraction and determination of melamine in milk and feed using gas chromatography-mass spectrometry. **878:** 2333-2338.

[10] R. Mirzajani, Z. Ramezani, F. Kardani. **2017**, *Microchem J.* Selective determination of thidiazuron herbicide in fruit and vegetable samples using molecularly imprinted polymer fiber solid phase microextraction with ion mobility spectrometry detection (MIPF-SPME-IMS). **130:** 93-101.

[11] I.D. Souza, L.P. Melo, I.C.S.F. Jardim, J.C.S. Monteiro, A.M.S. Nakano, M.E.C. Queiroz. **2016**, *Anal Chim Acta*. Selective molecularly imprinted polymer combined with restricted access material for in-tube SPME/UHPLC-MS/MS of parabens in breast milk samples. **932:** 49-59.

[12] C.M.B. María, N.V. Fernando, B.P. Elena, L.U. Javier. **2008**, *Curr Anal Chem.* Molecularly imprinted polymers as selective recognition elements in optical sensing. **4:** 316-340.

[13] X. Song, J. Wang; J. Zhu, **2009,** *Mat Res.* Effect of porogenic solvent on selective performance of molecularly imprinted polymer for quercetin. **12:** 299-304.

[14] A.S. Dorcheh, M.H. Abbasi. **2008,** *J Mater Process Technol*. Silica aerogel; synthesis, properties and characterization. **199:** 10-26.

[15] Y.S. Chang, T.H. Ko, T.J. Hsu, M.J. Syu. **2009**, *Anal Chem.* Synthesis of an imprinted hybrid Organic-inorganic polymer sol-gel matrix toward the specific binding and isotherm kinetics investigation of creatinine. **81:** 2098–2105.

[16] W.A.W. Ibrahim, K.V. Veloo, M.M. Sanagi. **2012**, *J Chromatogr A*. Novel sol-gel hybrid methyltrimethoxysilane-tetraethoxysilane as solid phase extraction sorbent for organophosphorus pesticides. **1229:** 55- 62.

[17] M. Polyakov; Z. Khim. **1931**, *Zh. Fiz.* Khim., Adsorption properties of silica gel and its structure. **2:** 799.

[18] F. H. Dickey. **1949**, *Proc. Natl. Acad. Sci. U.S.A.* The preparation of specific adsorbents. **35:** 227.

[19] C. Wenjing, L. Zhujuan, W. Yan. **2013**, *Talanta*, Preparation and application of surface molecularly imprinted silica gel for selective extraction of melamine from milk samples, **116:** 396-402.

[20] D. Yua, Y. Zenga, Y. Qia, T. Zhouc, G. Shia. **2012**, *Biosens Bioelectron*. A novel electrochemical sensor for determination of dopamine based on AuNPs@ SiO_2 core-shell imprinted composite. **38:** 270–277.

[21] J. Liu, H. Song, J. Liu, Y. Liu, L. Li, H. Tang, Y. Li. **2015**, *Talanta*, Preparation of molecularly imprinted polymer with double templates for rapid simultaneous determination of melamine and dicyandiamide in dairy products. **134:** 761–767.

[22] L. Zhu, G. Xu, F. Wei, J. Yang, Q. Hu. **2015**, J Colloid Interf Sci. Determination of melamine in powdered milk by molecularly imprinted stir bar sorptive extraction coupled with HPLC. **454:** 8-13.

[23] D. He , X. Zhang, B. Gao, L. Wang, Q. Zhao, H. Chen, H. Wang, C. Zhao. **2014**, *Food Control*. Preparation of magnetic molecularly imprinted polymer for the extraction of melamine from milk followed by liquid chromatography-tandem mass spectrometry. **36**: 36-41.

[24] T. Yamabe, K. Akagi, T. Hashimoto, S. Nagata, K. Fuku, **1977**, J. Chem. Soc., Faraday Trans. I. Hydrogen Bonding Type Charge Transfer Interaction between Thiols and Amines. **73:** 1860-1869.
[25] G. C. Pimentel and A. L. Mc Clellan, *The Hydrogen Bond* (Freeman, San Francisco, 1960) (Hydrogen bonding1)
[26] R. Bicca de Alencastro and C. Sandorfy, Canad. J. Chem., 1972, 50, 3594 ; 1973, 51,985.
[27] A.O. Dadda, A.P. Olalekan, A.M. Olatunya, O. Dadda, **2012**, *J App Chem*. Langmuir, Freundlich, Temkin and Dubinin–Radushkevich isotherms studies of equilibrium sorption of Zn^{2+} unto Phosphoric Acid modified rice husk. **3:** 38-45.
[28] Y.S. Li, Y.Wang, T. Tran, A. Perkins, **2005**, *Spectrochim Acta Part A*. Vibrational spectroscopic studies of (3-mercaptopropyl)trimethoxysilane sol-gel and its coating. **61:** 3032-3037.
[29] K.Z. El Wakeel, S. El-Kousy, H.G. El-Shorbagy, M.A. Abd El.Ghaffar, **2016**, *J Environ Eng*. Comparison between the removal of Reactive Black 5 from aqueous solutions by 3‑amino‑1,2,4 triazole, 5‑thiol and melamine grafted chitosan prepared through four different routes. **4:** 733‑745.
[30] C. Kulsing, R. Knob, M. Macka, P. Junor, R.I. Boysen, M.T.W Hearn, **2014**, *J Chromatogr A*. Molecular imprinted polymeric porous layers in open tubular capillaries for chiral separations. **1354:** 85-91.
[31] J. Fan, W. Cai, J. Yu, **2011**, *Chem Asian J*. Adsorption of N719 dye on anatase TiO_2 nanoparticles and nanosheets with exposed (001) facets: Equilibrium, kinetic, and thermodynamic studies. **6:** 2481–2490.
[32] I.A.W. Tan, B.H. Hameed, **2010**, *J Appl Sci*. Adsorption Isotherms, Kinetics, Thermodynamics and Desorption Studies of Basic Dye on Activated Carbon Derived from Oil Palm Empty Fruit Bunch, **10:** 2565-2571.
[33] K. Mohanty, D. Das, M.N. Biswas, **2005**, *Chem Eng J*. Adsorption of phenol from aqueous solutions using activated carbons prepared from Tectona grandis sawdust by $ZnCl_2$ activation. **115:** 121-131.
[34] C.H. Giles, A.P. D'Silva, I.A. Easton, **1973**, *J Colloid Interf Sci*. A general and classification of the solute adsorption isotherm. **47:** 766-778.
[35] S.Y. Shi, J.F. Guo, Q.P. You, X.Q. Chen, Y.P. Zhang, **2014**, *Chem Eng*. Selective and simultaneous extraction and determination of hydroxybenzoic acids in aqueous solution by magnetic molecularly imprinted polymers. **243:** 485-493.
[36] Z. Sun, W. Schussler, M. Sengl, R. Niessner, D. Knopp. **2008**, *Anal Chim Acta*. Selective trace analysis of diclofenac in surface and wastewater samples using solid-phase extraction with a new molecularly imprinted polymer. **620:** 73-81.